

# MESUREMENT OF LOCAL CONVECTIVE SURFACE HEAT TRANSFER COEFFICIENT BY PHOTOELECTRIC METHOD

Peter Mihalka, Milan Drzik, Peter Matiasovsky

*Institute of Construction and Architecture, Slovak Academy of Sciences,  
Dubravská cesta 9, 845 03 Bratislava 45, Slovakia, usarmipe@savba.sk*

## Abstract:

The surface transport coefficients modelling in complex models of the heat, air and moisture transport in a building supposes the local modelling of internal surface heat transfer in a hygrothermal zone. For this purpose the algorithm has been created for iterative computational determination of local convective surface heat transfer coefficients by CFD simulation tool. The convective surface heat transport coefficients determined by the algorithm were tested by experimental measurements for chosen surfaces configurations with use of the photoelectric measurements of the air refractive index gradient in a boundary layer.

## Keywords:

boundary layer, convective heat transfer coefficient, photoelectric method

## 1. INTRODUCTION

In order to evaluate the heat transfer coefficient a method of photoelectric probing of the refractive index gradients has been developed. The boundary layer was mapped in detail, the temperature gradients and temperatures were determined and approximated with an analytical solution for the laminar convection regime and then compared with a results simulated by a CFD tool.

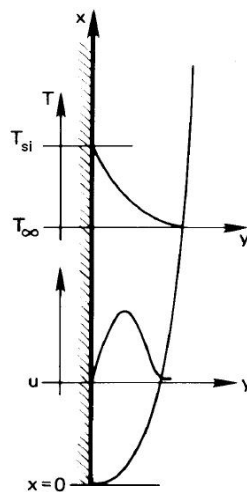


Fig. 1 Heat transfer and fluid flow near heated vertical plate

## 2. THEORY

The wall surface convective heat flux can be defined by the empirical Newton law [4]:

$$q = h.(\theta_{si} - \theta_{\infty}) \quad (1)$$

where  $h$  is the surface heat transfer coefficient.

The density of steady-state heat flow is determined by the Fourier law of heat conduction [4]:

$$q = -\lambda. \frac{d\theta}{dy} \quad (2)$$

where:  $dT/dy$  is the temperature gradient along the  $y$ -axis,  $\lambda$  is the thermal conductivity of air.

Using the equations (1) and (2) the value of convective heat transfer coefficient can be evaluated [4]:

$$h = \frac{-\lambda \cdot \left. \frac{d\theta}{dy} \right|_{y=0}}{\theta_{si} - \theta_{\infty}} \quad (3)$$

The experimental determination of the temperature gradient is based on the relationship between the air density dependent on the air temperature and refractive index. This relation is described by the Lorenz-Lorentz law [1]:

$$\frac{n^2 - 1}{n^2 + 2} \cdot \frac{1}{\rho} = \frac{N}{M} = const. \quad (4)$$

where:  $n$  is the air refractive index [-],  $\rho$  is the air density [ $\text{kg/m}^3$ ],  $N$  is the air molar refraction [ $\text{m}^3/\text{mol}$ ],  $M$  is the air molar mass [ $\text{g/mol}$ ]

The refractive index for a current light wavelength is a function of the air density [1]:

$$n = n(\rho) \quad (5)$$

In the range of 300 – 400 K and under the atmospheric pressure the air can be regarded as an ideal gas. The dependence between air density and temperature is given by the state equation [1]

$$\frac{p.V}{T} = R \quad \text{i.e.} \quad \rho = \frac{p.M}{R.T} \quad (6)$$

where:  $p$  is the air pressure [Pa],  $T$  is the absolute temperature [K],  $V$  is the air molar volume [ $\text{m}^3/\text{mol}$ ],  $R$  is the universal gas constant [ $\text{J/mol.K}$ ].

Under the assumption of isobaric condition, the air density change is proportional inversely to the temperature change, then the refractive index variation is proportional to the air temperature change [1]:

$$\frac{n_0 - 1}{n - 1} = \frac{\rho_0}{\rho} = \frac{T}{T_0} \quad (7)$$

In a literature the basic constant can be found for the relationship between air temperature change and refractive index change for the wavelength of 650 nm at the temperature of 300 K [1]:

$$\frac{dn}{dT} = 0.961 \cdot 10^{-6} \quad (8)$$

Then, the mutual relationship between the refractive index gradients and temperature gradients is as follows:

$$\frac{dT}{dy} = \frac{1}{0.961 \cdot 10^{-6}} \cdot \frac{dn}{dy} \quad (9)$$

Considering the constant distribution of refractive index along the path of optical detection by laser beam and appropriate geometrical relations, a final equation for beam deviation in the detector place is [2, 3]:

$$\frac{\partial n}{\partial y} = \frac{2 \cdot n_0 \cdot \Delta y}{L^2} \quad (10)$$

where:  $L$  is the laser beam path length [m],  $n_0$  is the refractive index  $\cong 1.0$  for air,  $\Delta y$  is the laser beam deviation.

With use of the equations (10) and (9) the wall temperature gradient near a wall surface and then the near wall temperature profile has been evaluated. Finally, applying the equations (10), (9) and (3) the convective heat transfer coefficients can be computed.

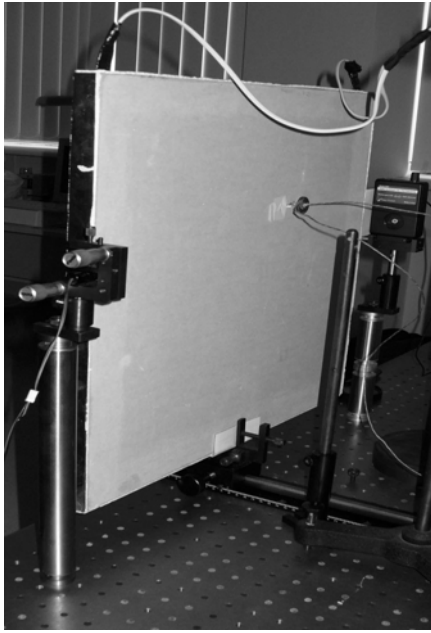
### 3. EXPERIMENT

For the purpose of experiment the vertical flat plates consisting of two symmetrically heated parts has been fabricated. Two materials with different thermal conductivity were used. In the first case the plate consisted of two gypsum boards (G) with the embedded heating foil the dimensions of which were 0.52 x 0.50 x 0.02 m. In the second case the gypsum boards were replaced by the polished aluminium plates (A) with dimensions of 0.5 x 0.5 x 0.09 m. The foil heating input was 197 W/m<sup>2</sup> at 220 V.

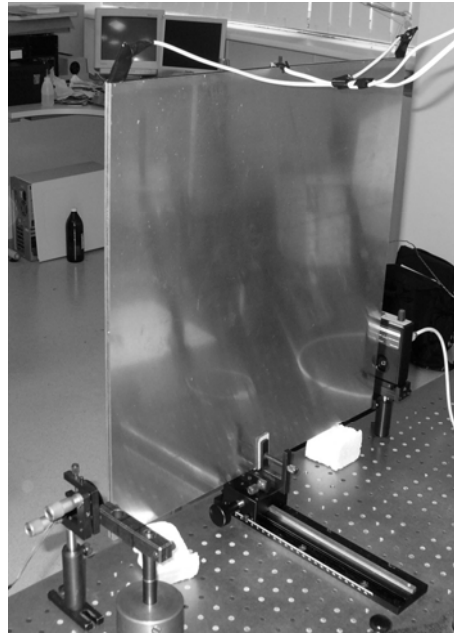
In a case of the gypsum plate with relatively low thermal conductivity (0.15 W/m.K) some heterogeneity of the surface temperature field was expected. The perimeter of the plate was therefore thermally insulated with the 0.003m thick expanded polystyrene belt and aluminium foil. The gypsum plate was used at the experiments with higher surface-ambient temperature differences.

The aluminium plate has a significantly higher thermal conductivity (204 W/m.K) providing a higher homogeneity of surface temperature field. This plate was applied at experiments with low surface-ambient temperature differences.

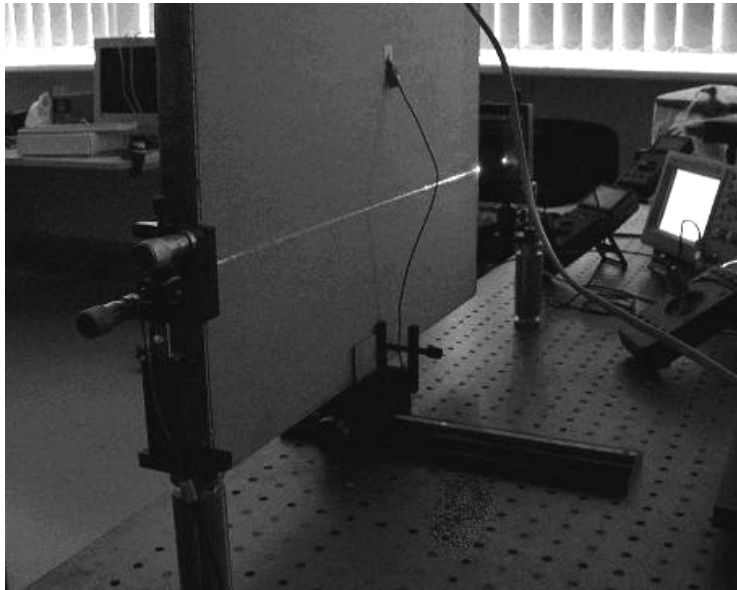
The configuration of measurement equipment is shown in figure 2. The laser source in the figure is in the position  $y = 0$  mm, thus the laser beam is visible on the plate surface (at bottom).



a



b



c

Fig. 2 Image of measurement set up: a – surface G (gypsum boards), b – surface A (aluminium plates), c - laser beam illuminating heated wall

The measurement set consists of the laser diode 10 mW/650 nm (Fig. 3 a) with the wavelength of light 650 nm and the double photodiode detector (Fig. 3 b). The air and surface temperatures were measured by thermocouples and in a case of gypsum plate also with the infrared camera NEC TH7102MX. The thermocouples sensitivity was  $0.1^{\circ}\text{C}$ .

Under the calm air conditions with the absence of temperature gradient and dominant air speed, the laser beam impacts both halves of the photodiode detector equally. If the air temperature gradient occurs, the air density decreases, the laser beam deviates from a straight line and the photodiode

captures the difference between the two laser detecting halves (Fig. 4 b). This difference is observed by the voltmeter and is proportional to the deviation of beam from a straight line.

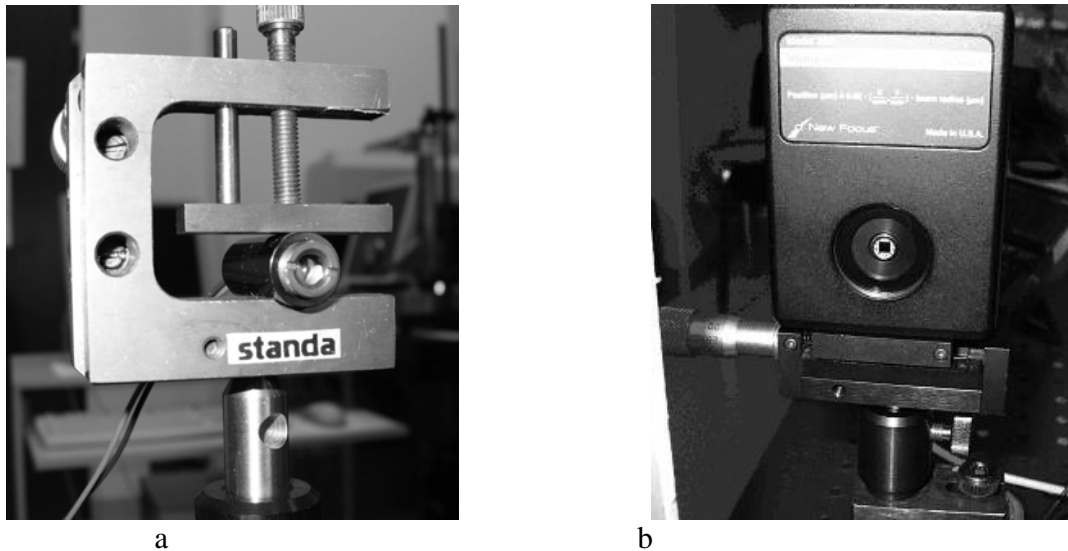


Fig. 3 Measurement apparatus  
 a – laser diode, b – double photodiode detector with screw micrometer

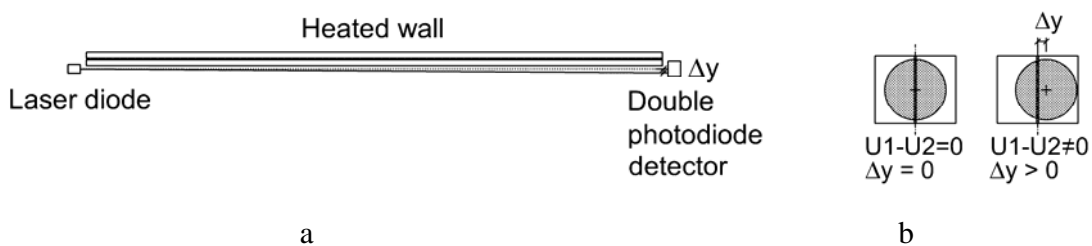


Fig.4 Principle of laser beam deviation measurement  
 a – laser beam deviation along the heated vertical plate, b – laser beam impact onto the double photodiode, left image - with no temperature gradient, right image - with temperature gradient

During the measurements the laser diode and photodiode detectors had a fixed position and the heated plate was moved in defined steps using a screw micrometer. The values of the gradients signal were read after the air consolidation.

The adjustment of the state  $dn/dy = 0$  was made by the moving of the heated plate outside the boundary layer and by using the screw micrometer at the double photodiode detector. The calibration of the relation between mV and  $\mu\text{m}$  then can be reached.

The measurements were made within the distances from  $y = 0.002$  up to  $0.026$  m. The measurements at smaller distances were not possible as the smallest distance is limited due to a finite laser beam diameter (about  $0.0015$  m) and also by the fact that the heated plate surfaces were not ideally flat.

The evaluation process assumes the constant temperature gradient along the heated plate. In fact, there was not possible to keep the constant distribution of surface temperature along the whole gypsum plate area (Fig. 5 a). A correction of the path length along the heated plate was necessary (Fig. 5 b)

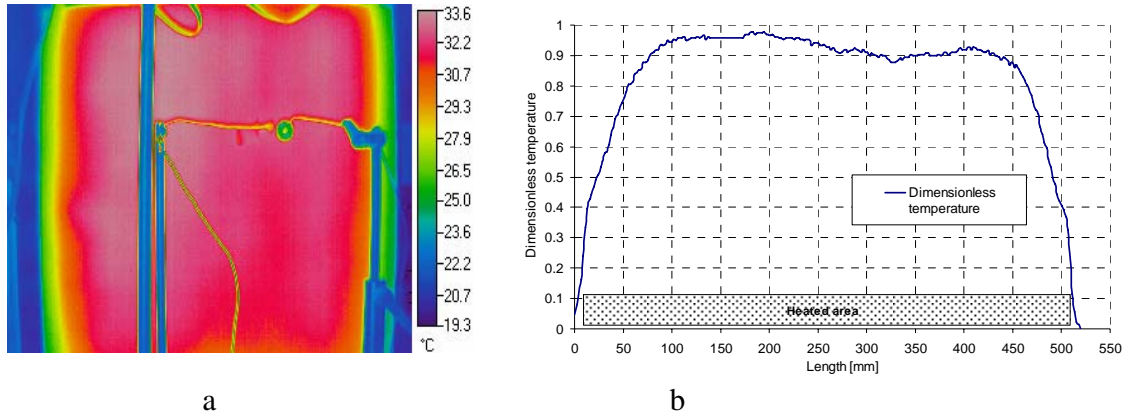


Fig. 5 Surface temperature variation along laser beam path (plate G): a – thermography, b- temperature profile along laser beam

The correction was made by integrating the temperature profile along laser beam path what represents area of temperature profile function. Dividing the integrated temperature profile by average temperature, the corrected laser beam path length can be evaluated.

$$L = \frac{a}{t_{average}} \int_a^b t(x) dx \quad (11)$$

where  $a$  and  $b$  are coordinates of the beginning and the end of the plate. Applying equation (11) the corrected laser beam path length 0.49 m was obtained.

#### 4. RESULTS

The measured results were compared with known analytical solutions of the natural convection along the vertical plate [2], [3]. The measured temperature gradients courses were approximated by Gauss regression the shape (15):

$$\frac{d\theta}{dy} = a + b \cdot e^{-\left(\frac{y-c}{d}\right)^2} \quad (12)$$

where the parameters  $a$ ,  $b$ ,  $c$ ,  $d$  determined by the regression.

Subsequently the function of temperatures near the plate could be obtained by the integration of function  $d\theta/dy$ :

$$\theta(y) = \int \frac{d\theta}{dy} dy = a \cdot y + \frac{1}{2} \pi^{\frac{1}{2}} \cdot d \cdot \operatorname{erf}\left(\frac{y}{d} - \frac{c}{d}\right) \cdot b + C \quad (13)$$

where  $C$  is the integration constant, which has for  $y = 0$  has the value  $\theta_{si}$ :

$$C = \theta_{si} + \frac{1}{2} \cdot \pi^{\frac{1}{2}} \cdot d \cdot \operatorname{erf}\left(-\frac{c}{d}\right) \cdot b \quad (14)$$

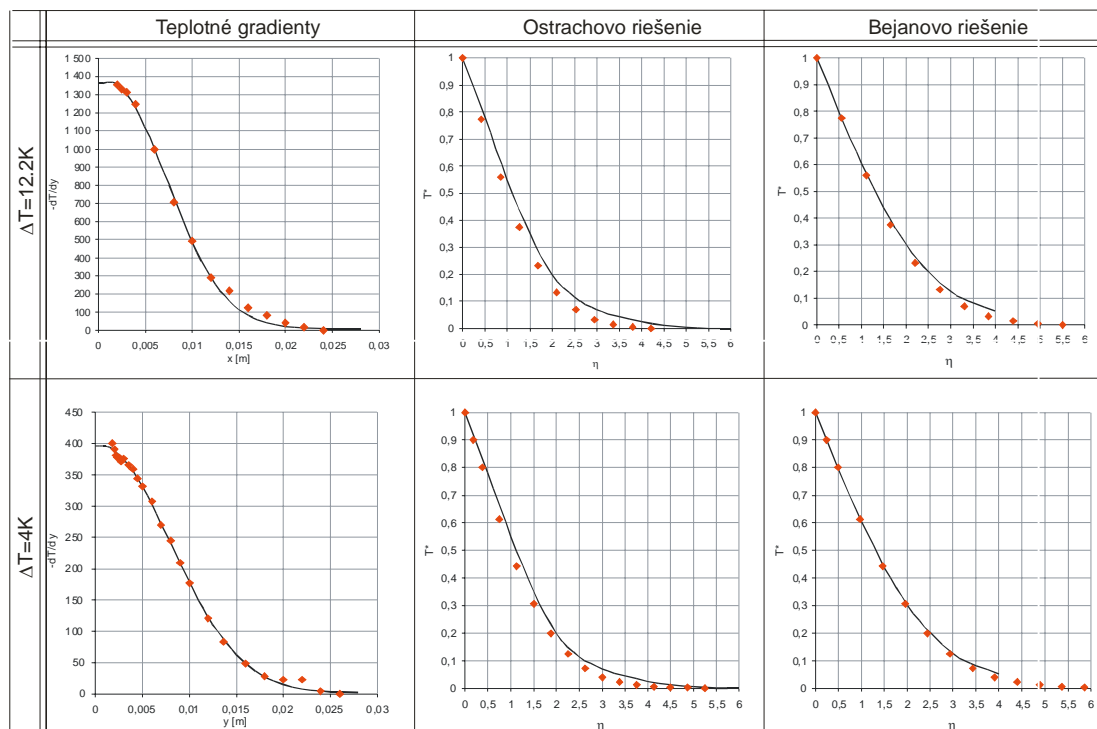


Fig. 6 Results of measurements compared with analytical solutions

The comparison of measured and calculated temperature profiles is in figure 6. From the comparison of measured and calculated results a good agreement is evident. The straight comparison of the obtained values with known empirical relationships is not possible, as the obtained values are local character, determined by not only the temperature difference but also the spatial coordinates.

## 5. CONCLUSIONS

The photoelectric method enables to measure the temperature gradients in a boundary layer, using the temperature dependence of light refractive index in air. In comparison with other methods the errors at the measured temperature profile derivations are limited. Potential inaccuracies are caused by the forced convection of ambient air. The method is applicable for measurements at low temperature differences.

### Acknowledgement

Financial support of the project APVT-51-030704 is gratefully acknowledged.

### REFERENCES

- [2] FOMIN, N.A. (1989): Speckle interferometrija gazovykh potokov, Nauka I tehnika, Minsk (in Russian)
- [3] VASILJEV, L.A. (1968): Tenevije metody, Nauka, Moscow (in Russian)
- [4] CHAPMAN, A.J. (1960): Heat transfer, The Macmillan Company, New York
- [5] SCHLICHTING, H. (1979): Boundary-Layer theory, McGraw-Hill7